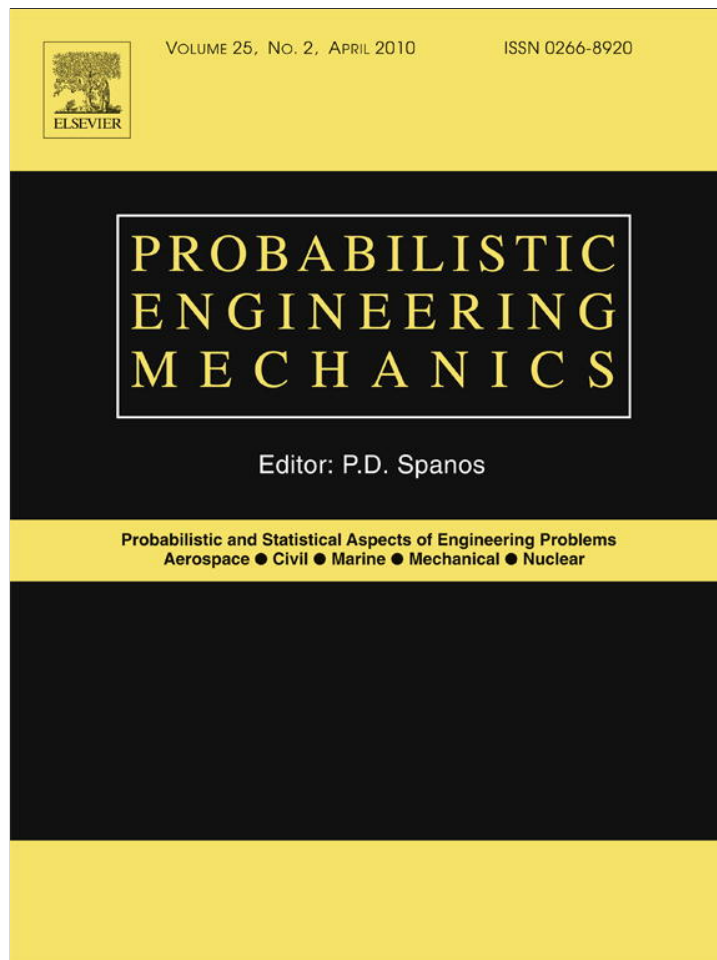


Provided for non-commercial research and education use.  
Not for reproduction, distribution or commercial use.



This article appeared in a journal published by Elsevier. The attached copy is furnished to the author for internal non-commercial research and education use, including for instruction at the authors institution and sharing with colleagues.

Other uses, including reproduction and distribution, or selling or licensing copies, or posting to personal, institutional or third party websites are prohibited.

In most cases authors are permitted to post their version of the article (e.g. in Word or Tex form) to their personal website or institutional repository. Authors requiring further information regarding Elsevier's archiving and manuscript policies are encouraged to visit:

<http://www.elsevier.com/copyright>



Contents lists available at ScienceDirect

# Probabilistic Engineering Mechanics

journal homepage: [www.elsevier.com/locate/probengmech](http://www.elsevier.com/locate/probengmech)

## Stochastic finite element analysis of a cable-stayed bridge system with varying material properties

Özlem Çavdar<sup>a</sup>, Alemdar Bayraktar<sup>b,\*</sup>, Süleyman Adanur<sup>b</sup>

<sup>a</sup> Gumushane University, Department of Civil Engineering, 29000, Gumushane, Turkey

<sup>b</sup> Karadeniz Technical University, Department of Civil Engineering, 61080, Trabzon, Turkey

### ARTICLE INFO

#### Article history:

Received 8 February 2008

Received in revised form

18 January 2010

Accepted 26 January 2010

Available online 1 February 2010

#### Keywords:

Stochastic finite element method (SFEM)

Stochastic perturbation technique

Cable-stayed bridge

Random variable

Monte Carlo simulation (MCS) method

### ABSTRACT

Stochastic seismic finite element analysis of a cable-stayed bridge whose material properties are described by random fields is presented in this paper. The stochastic perturbation technique and Monte Carlo simulation (MCS) method are used in the analyses. A summary of MCS and perturbation based stochastic finite element dynamic analysis formulation of structural system is given. The Jindo Bridge, constructed in South Korea, is chosen as a numerical example. The Kocaeli earthquake in 1999 is considered as a ground motion. During the stochastic analysis, displacements and internal forces of the considered bridge are obtained from perturbation based stochastic finite element method (SFEM) and MCS method by changing elastic modulus and mass density as random variable. The efficiency and accuracy of the proposed SFEM algorithm are evaluated by comparison with results of MCS method. The results imply that perturbation based SFEM method gives close results to MCS method and it can be used instead of MCS method, especially, if computational cost is taken into consideration.

© 2010 Elsevier Ltd. All rights reserved.

### 1. Introduction

Bridges with very long spans have always been a great challenge for engineers throughout history. Cable-stayed types of bridges are becoming more and more popular in the construction of long span bridges due to their many advantages, i.e. light in weight, efficient in load resistance, and of smaller cross sections. Cable-stayed bridges which consist of main girders, towers and cables are complicated structures. From these towers, cables stretch down diagonally and support the girder. Cable-stayed bridge can be distinguished by the number of spans, number of towers, girder type, number of cables and types of cables. The cable-stayed bridge can be constructed for even longer spans, if the deck and cable stiffness and strength to weight ratios can be improved. This could significantly diminish the critical compressive stresses of the deck in the tower zones, and increase the apparent stiffness of the stay-cables, as their sag action is reduced due to a huge drop of the weight per unit length.

The traditional structural analyses are realized according to the assumption that geometrical and material characteristics of structures are deterministic. However, there are some uncertainties about design values. These uncertainties can be defined as geometrical characteristics (cross-sectional area, flexural inertia,

length etc.), material characteristics (elastic modulus, Poisson's ratio, mass density etc.), and magnitudes and distributions of the loads. The deterministic method could be disqualified for many structural system analyses because of these uncertainties. MCS is the most employed method among the stochastic analysis methods for structural problems. It lies on the generation of a defined number of samples of the uncertain parameters and on the solution of the corresponding deterministic problems. However, as the number of degrees of freedom of the structure and the number of uncertain parameters increase, structural analyses with the Monte Carlo become very heavy from a computational point of view, and, in some cases, the computational effort makes them inapplicable. Accordingly, some non-statistical alternative procedures have been proposed in the literature [1–5]. On the other hand, stochastic finite element method (SFEM), which is one of the probabilistic analysis methods, increases its reliability day by day. Most of them are based on perturbation techniques, so that the SFEM is often identified as the classical finite element method (FEM) coupled with a perturbation approach. This method is applied several field in civil engineering, especially, simple or semi-complex structure systems.

Although there is an extensive literature on deterministic analysis of bridges [6–9], technical literature is not adequate on the stochastic dynamic analysis of cable-stayed bridge. The dynamic behaviors of cable-stayed bridges have been studied by several researchers [10,11]. Linear and nonlinear static and earthquake-response analyses of cable-stayed bridges were carried out by many researchers [12–15] only in the past two decades.

\* Corresponding author. Tel.: +90 462 377 26 53; fax: +90 462 377 26 06.

E-mail addresses: [ozlem\\_cavdar@hotmail.com](mailto:ozlem_cavdar@hotmail.com) (Ö. Çavdar), [alemdar@ktu.edu.tr](mailto:alemdar@ktu.edu.tr) (A. Bayraktar), [sadanur@ktu.edu.tr](mailto:sadanur@ktu.edu.tr) (S. Adanur).

The SFEM algorithm for structures has been developed by several researchers [16–20]. However, most of their work is limited to simple structures. More complex structures such as cable-stayed bridges are not considered. Very few researchers [21–23] studied the stochastic finite element method with random variable material and geometrical properties of cable-stayed bridges. Cheng and Xiao [22] proposed a stochastic finite-element-based algorithm for the probabilistic free vibration and flutter analysis of suspension bridges through combination of the advantages of the response surface method, FEM and MCS. Liu et al. [23] investigated large flexible structures, such as suspension bridges, actually possess stochastic material properties and these random properties unavoidably affect the dynamic system parameters. It is concluded from numerical analysis of a modern suspension bridge that although the second-order statistics of frequencies are small relatively to the change of basic design variables, such as density of mass and modulus of elasticity, the sensitivities of modal parameters to these variables at different locations change in magnitude.

The focus of the present paper is to perform the stochastic dynamic analysis of a cable-stayed bridge by using the perturbation based SFEM and MCS methods. During stochastic analysis, displacements and internal forces of the systems are obtained from perturbation based SFEM and MCS methods by using different uncertainties of material characteristics. Elastic modulus and mass density are chosen as random variable material properties. The analysis results obtained from these two methods are compared with each other.

## 2. Stochastic finite element method (SFEM)

In the stochastic finite element method (SFEM), the deterministic finite element formulation is modified using the perturbation technique or the partial derivative method to incorporate uncertainties in the structure systems. Since the basic variables are stochastic, every quantity computed during the deterministic analysis, being a function of the basic variables, is also stochastic. Therefore, the efficient way to arrive at the stochastic response may be to keep account of the stochastic variation of the quantities at every step of the deterministic analysis in terms of the stochastic variation of the basic variables.

A SFEM, which is based on perturbation technique, is developed. The method developed here uses an alternate approach for obtaining improved computational efficiency. The derivatives of the concentration with respect to random parameters are obtained by using the derivatives of local matrices instead of global matrices. This approach increases the computational efficiency of the present method by several orders with respect to standard SFEM. There are two fundamental ways to solve the stochastic problem (i) analytical approach and (ii) numerical approach. Among analytical approaches, the perturbation method is widely used because of its simplicity. Numerical method such as Monte Carlo Simulation is generally applicable to all types' stochastic problems and is often used to verify the results obtained from analytical methods. A detailed discussion of these methods is presented below.

### 2.1. Perturbation based SFEM formulation

The perturbation method is the most widely used technique for analyzing uncertain system. This method consists of expanding all the random variables of an uncertain system around their respective mean values via Taylor series and deriving analytical expression for the variation of desired response quantities such as natural frequencies and mode shapes of a structure due to small variation of those random variables. The basic idea behind the perturbation method is to express the stiffness and mass matrices and the responses in terms of Taylor series expansion with respect to the parameters centered at the mean values.

Since the deterministic equations are valid for the MCS analysis as well, then the essential differences are observed in case of perturbation based stochastic finite element analysis. Let us consider a deterministic equation of motion in the form of

$$M\ddot{q} + C\dot{q} + Kq = Q_\alpha \quad (1)$$

where  $K$ ,  $M$ ,  $C$  denote the stiffness matrix, mass matrix and damping matrix,  $\ddot{q}$ ,  $\dot{q}$ ,  $q$  denote the acceleration, velocity, displacement, respectively. The stochastic perturbation based approach consists usually of up to the second-order equations obtained starting from the deterministic ones.

The basic idea of the mean based, second-order, second-moment analysis in stochastic finite element moment is to expand, via Taylor series, all the vector and matrix stochastic field variables typical of deterministic finite element method about the mean values of random variables ( $b$ ), to retain only up to second-order terms and to use in the analyses only the first two statistical moments. In this way equations for the expectations and covariances of the nodal displacements can be obtained in terms of the nodal displacement derivatives with respect to the random variables.

The perturbation stochastic finite element equations describing dynamic response of random variable system for zeroth, first and second order:

Zeroth-order equation ( $\epsilon^0$  terms, one system of  $N$  linear simultaneous ordinary differential equations for  $q_\alpha(b; \tau)$ ,  $\alpha = 1, 2, \dots, N$ )

$$M(b)\ddot{q}(b; \tau) + C(b)\dot{q}(b; \tau) + K(b)q(b; \tau) = Q_\alpha(b; \tau). \quad (2)$$

First-order equations, rewritten separately for all random variables of the problem ( $\epsilon^1$  terms,  $\bar{N}$  systems of  $N$  linear simultaneous ordinary differential equations for  $q_\alpha^\rho(b; \tau)$ ,  $\rho = 1, 2, \dots, \bar{N}$ ,  $\alpha = 1, 2, \dots, N$ )

$$M(b)\ddot{q}^\rho(b; \tau) + C(b)\dot{q}^\rho(b; \tau) + K(b)q^\rho(b; \tau) = Q_\alpha^\rho(b; \tau) - [M^{\cdot\rho}(b)\ddot{q}^0(b; \tau) + C^{\cdot\rho}(b)\dot{q}^0(b; \tau) + K^{\cdot\rho}(b)q^0(b; \tau)]. \quad (3)$$

Second-order ( $\epsilon^2$  terms, one system of  $N$  linear simultaneous ordinary differential equations for  $q_\alpha^2(b; \tau)$ ,  $\alpha = 1, 2, \dots, N$ )

$$M(b)\ddot{q}^{(2)}(b; \tau) + C(b)\dot{q}^{(2)}(b; \tau) + K(b)q^{(2)}(b; \tau) = \left\{ Q_\alpha^{\rho\sigma}(b; \tau) - 2[M^{\cdot\rho}(b)\dot{q}^{\cdot\sigma}(b; \tau) + C^{\cdot\rho}(b)\dot{q}^\sigma(b; \tau) + K^{\cdot\rho}(b)q^\sigma(b; \tau)] - [M^{\cdot\rho\sigma}(b)\ddot{q}^0(b; \tau) + C^{\cdot\rho\sigma}(b)\dot{q}^0(b; \tau) + K^{\cdot\rho\sigma}(b)q^0(b; \tau)] \right\} S_b^{\rho\sigma} \quad (4)$$

where

$$q_\alpha^{(2)}(b; \tau) = q_\alpha^{\rho\sigma}(b; \tau) S_b^{\rho\sigma} \quad (5)$$

where  $b$  is the vector of nodal random variables,  $q_\alpha$  is the vector of nodal displacement-type variables,  $\tau$  is forward time variable,  $\bar{N}$  is the number of nodal random variables.  $M$ ,  $C$  and  $K$  are system mass matrix, damping matrix and system stiffness matrix, respectively.  $Q_\alpha$ ,  $q$  and  $S_b^{\rho\sigma}$  are load vector, displacement and the covariance matrix of the nodal random variable, respectively.  $N$  is the number of degrees of freedom in the system.  $(\cdot)^0$  is zeroth-order quantities, taken at means of random variables,  $(\cdot)^\rho$  is first partial derivatives with respect to nodal random variables,  $(\cdot)^{\rho\sigma}$  is second partial derivatives with respect to nodal random variables.

In Eqs. (2)–(4) the zeroth-order mass, damping and stiffness matrices and local vector and their first and second mixed derivatives with respect to nodal random variables  $b_\ell$  are defined as follows;

Zeroth-order functions

$$M(b) = \int_\Omega \varphi_\alpha \ell_\alpha^0 \varphi_{i\alpha} \varphi_{i\beta} d\Omega \quad (6)$$

$$C(b) = \int_\Omega \varphi_\alpha \varphi_\beta (\varphi_\alpha^0 \ell_\beta^0 \varphi_{i\alpha} \varphi_{i\beta} + \beta_\alpha^0 C_{ijkl}^0 B_{ij\alpha} B_{kl\beta}) d\Omega \quad (7)$$

$$K(b) = \int_{\Omega} \varphi_{\bar{\alpha}} C_{ijkl\bar{\alpha}}^0 B_{ij\alpha} B_{kl\beta} d\Omega \quad (8)$$

$$Q_{\alpha}(b; \tau) = \int_{\Omega} \varphi_{\bar{\alpha}} \varphi_{\bar{\beta}} \ell_{\alpha\beta}^0 f_{i\beta}^0 \varphi_{i\alpha} d\Omega + \int_{\partial\Omega\sigma} \varphi_{\bar{\alpha}} \hat{t}_{i\alpha}^0 \varphi_{i\alpha} d(\partial\Omega). \quad (9)$$

First partial derivatives

$$M^{\cdot\rho}(b) = \int_{\Omega} \varphi_{\bar{\alpha}} \ell_{\bar{\alpha}}^{\cdot\rho} \varphi_{i\alpha} \varphi_{i\beta} d\Omega \quad (10)$$

$$C^{\cdot\rho}(b) = \int_{\Omega} \varphi_{\bar{\alpha}} \varphi_{\bar{\beta}} [(\alpha_{\bar{\alpha}}^{\cdot\rho} \ell_{\bar{\beta}}^0 + \alpha_{\bar{\alpha}}^0 \ell_{\bar{\beta}}^{\cdot\rho}) \varphi_{i\alpha} \varphi_{i\beta} + (\beta_{\bar{\alpha}}^{\cdot\rho} C_{ijkl\bar{\beta}}^0 + \beta_{\bar{\alpha}}^0 C_{ijkl\bar{\beta}}^{\cdot\rho}) B_{ij\alpha} B_{kl\beta}] d\Omega \quad (11)$$

$$K^{\cdot\rho}(b) = \int_{\Omega} \varphi_{\bar{\alpha}} C_{ijkl\bar{\alpha}}^{\cdot\rho} B_{ij\alpha} B_{kl\beta} d\Omega \quad (12)$$

$$Q_{\alpha}^{\cdot\rho}(b; \tau) = \int_{\Omega} \varphi_{\bar{\alpha}} \varphi_{\bar{\beta}} (\ell_{\bar{\alpha}}^{\cdot\rho} f_{i\beta}^0 + \ell_{\bar{\alpha}}^0 f_{i\beta}^{\cdot\rho}) \varphi_{i\alpha} d\Omega + \int_{\partial\Omega\sigma} \varphi_{\bar{\alpha}} \hat{t}_{i\alpha}^{\cdot\rho} \varphi_{i\alpha} d(\partial\Omega). \quad (13)$$

Second partial derivatives

$$M^{\cdot\rho\sigma}(b) = \int_{\Omega} \varphi_{\bar{\alpha}} \ell_{\bar{\alpha}}^{\cdot\rho\sigma} \varphi_{i\alpha} \varphi_{i\beta} d\Omega \quad (14)$$

$$C^{\cdot\rho\sigma}(b) = \int_{\Omega} \varphi_{\bar{\alpha}} \varphi_{\bar{\beta}} [(\alpha_{\bar{\alpha}}^{\cdot\rho\sigma} \ell_{\bar{\beta}}^0 + \alpha_{\bar{\alpha}}^{\cdot\rho} \ell_{\bar{\beta}}^{\cdot\sigma} + \alpha_{\bar{\alpha}}^{\cdot\sigma} \ell_{\bar{\beta}}^{\cdot\rho} + \alpha_{\bar{\alpha}}^0 \ell_{\bar{\beta}}^{\cdot\rho\sigma}) \varphi_{i\alpha} \varphi_{i\beta} + (\beta_{\bar{\alpha}}^{\cdot\rho\sigma} C_{ijkl\bar{\beta}}^0 + \beta_{\bar{\alpha}}^{\cdot\rho} C_{ijkl\bar{\beta}}^{\cdot\sigma} + \beta_{\bar{\alpha}}^{\cdot\sigma} C_{ijkl\bar{\beta}}^{\cdot\rho} + \beta_{\bar{\alpha}}^0 C_{ijkl\bar{\beta}}^{\cdot\rho\sigma}) B_{ij\alpha} B_{kl\beta}] d\Omega \quad (15)$$

$$K^{\cdot\rho\sigma}(b) = \int_{\Omega} \varphi_{\bar{\alpha}} C_{ijkl\bar{\alpha}}^{\cdot\rho\sigma} B_{ij\alpha} B_{kl\beta} d\Omega \quad (16)$$

$$Q_{\alpha}^{\cdot\rho\sigma}(b; \tau) = \int_{\Omega} \varphi_{\bar{\alpha}} \varphi_{\bar{\beta}} (\ell_{\bar{\alpha}}^{\cdot\rho\sigma} f_{i\beta}^0 + \ell_{\bar{\alpha}}^{\cdot\rho} f_{i\beta}^{\cdot\sigma} + \ell_{\bar{\alpha}}^{\cdot\sigma} f_{i\beta}^{\cdot\rho} + \ell_{\bar{\alpha}}^0 f_{i\beta}^{\cdot\rho\sigma}) \varphi_{i\alpha} d\Omega + \int_{\partial\Omega\sigma} \varphi_{\bar{\alpha}} \hat{t}_{i\alpha}^{\cdot\rho\sigma} \varphi_{i\alpha} d(\partial\Omega). \quad (17)$$

All the functions (6)–(17) are evaluated at the expectations  $b$  of the nodal random variables  $b_{\ell}$ , where  $\Omega$  is angular Nyquist frequency,  $\partial\Omega$  is solid boundary,  $\varphi_{\bar{\alpha}}$  is random field shape function vector,  $\varphi_{i\alpha}$  is system shape function matrix,  $B_{ij\alpha}$  is strain–nodal displacement matrix and  $\ell$  is coefficient of correlation.  $C_{ijkl\bar{\alpha}}$ ,  $f_i$  and  $\hat{t}_i$  are constitutive tensor, vector of body forces and vector of boundary tractions, respectively.

The first two statistical moments for the random fields  $b_r(x_k)$ ,  $r = 1, 2, \dots, R$ , are defined as

$$E[b_r] = b_r^0 = \int_{-\infty}^{+\infty} b_r p_1(b_r) db_r \quad (18)$$

$$Cov(b_r, b_s) = S_b^{rs} = \int_{-\infty}^{+\infty} \int_{-\infty}^{+\infty} (b_r - b_r^0)(b_s - b_s^0) p_2(b_r, b_s) db_r db_s \quad (19)$$

$r, s = 1, 2, \dots, R$ .

The latter definition can be replaced by

$$S_b^{rs} = \alpha_{b_r} \alpha_{b_s} b_r^0 b_s^0 \mu_{b_r b_s} \quad (20)$$

with

$$\alpha_{b_r} = \left[ \frac{Var(b_r)}{b_r^0} \right]^{1/2} \quad (21)$$

$$\mu_{b_r b_s} = \int_{-\infty}^{+\infty} \int_{-\infty}^{+\infty} b_r b_s p_2(b_r, b_s) db_r db_s$$

where,  $E[b_r]$ ,  $Cov(b_r, b_s)$ ,  $Var(b_r)$  are the expectation value,

covariance and variance, respectively;  $\mu_{b_r b_s}$ ,  $\alpha_{b_r}$ ,  $p_1(b_r)$  are correlation functions, the coefficients of variation and probability density function (PDF), respectively.  $p_2(b_r, b_s)$  is the joint PDF.  $R$  is the random fields, which can represent randomness elastic modulus, and mass density the material.

All the equations, solved consequently for zeroth-, first- and second-order displacements, velocities and accelerations, make it possible to compute the first two probabilistic moments of the output in the form of expected values and cross-covariance's of the structural response.

## 2.2. Monte Carlo Simulation method

The MCS method is a quite versatile mathematical tool capable of handling situations where all other methods fail to succeed; in structural dynamics, it has attracted intense attention only recently following the widespread availability of inexpensive computational systems. This computational availability has triggered an interest in developing sophisticated and efficient simulation algorithms. Shinozuka [24] had a pioneering role in introducing the method to the field of structural dynamics. Shinozuka used the MCS for simulating a random process as the superposition of a large number of sinusoids having a uniformly distributed random phase angle. Zhang and Ellingwood [25] used this method to obtain the effects of random material properties. However, in most of the studies, the MCS was used to verify the results obtained from approximate methods [22,23].

The Monte Carlo Simulation generates a set of random values of  $X$  according to its probability distribution function. The set can be written as  $X = \{x_1, x_2, \dots, x_N\}$ , where  $N$  is the number of simulation. For each values of  $X$ , the stiffness and mass matrices are computed. At the end of  $N$  simulations, we have a random set of displacement and stress values  $\{\{q_{\beta}\}_1, \{q_{\beta}\}_2, \{q_{\beta}\}_3, \dots, \{q_{\beta}\}_N\}$ ,  $\{\{\sigma\}_1, \{\sigma\}_2, \{\sigma\}_3, \dots, \{\sigma\}_N\}$  for  $X_i$ . From this finite set of solutions, the expected values of displacement and stress are computed using the following formulas:

$$E\{q_{\beta}\} = \frac{1}{N} \sum_{i=1}^N \{q_{\beta}\}_i \quad (22)$$

$$E\{\sigma\} = \frac{1}{N} \sum_{i=1}^N \{\sigma\}_i. \quad (23)$$

## 3. Numerical application

The main objective of this work is to compare the behavior of two methodologies: perturbation techniques associated to the SFEM and MCS method; offering to the practicing engineers an overview of the techniques usually employed in the analysis of the uncertain parameters of a structural system. In this study, the comparison of the stochastic dynamic responses of a cable-stayed bridge system subject to ground motion is performed by using perturbation based SFEM and MCS methods. Displacements and other internal forces of the systems are obtained from methods mentioned above by using different uncertainties of material characteristics (elastic modulus and mass density) and compared with each other.

For this objective, the Jindo Bridge designed by Rendel Palmer and Tritton and built in South Korea is chosen as a practical example to investigate stochastic response of a cable-stayed bridge (Fig. 1). Jindo Bridge, which has three spans, the main span of 344 m and two side spans of 70 m (Fig. 2) subjected to earthquake ground motion (Fig. 3), is selected as an application for the generalized perturbation based stochastic finite element method. The stays are arranged in a fan configuration and converged at the



Fig. 1. Jindo cable-stayed bridge.

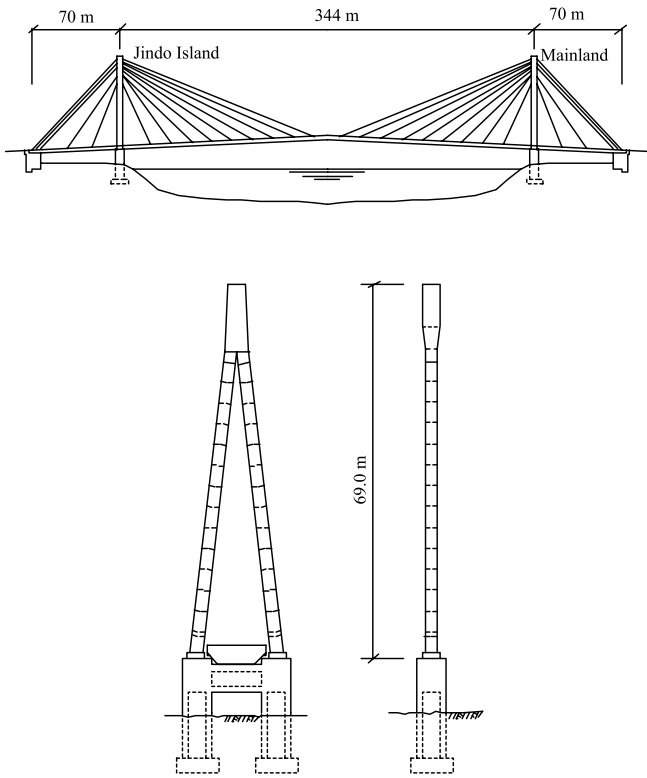


Fig. 2. General arrangements of the Jindo Bridge.

top of the A-frame towers. The diameters of the stays are 56 mm, 67 mm, 76 mm and 87 mm. Each tower carries 24 stays and the towers are 69 m height above the piers on which they are supported. Since a-frame towers are torsionally rigid, they have been preferred for many cable-stayed bridges. The stiffening girder is of a hexagonal shape and continues from one end to the other. The stiffening girder and the towers of the Jindo Bridge were made from steel [26]. A damping ratio of 2% is adopted for the response calculations of cable-stayed bridge. To investigate the dynamic responses of the Jindo Bridge, two-dimensional mathematical model is used for calculations (Fig. 2). It has been shown that a two-dimensional analysis of the cable-stayed bridge provides natural frequencies and mode shapes which are in close agreement with those obtained by three-dimensional analysis [27].

For the dynamic analysis, YPT330 component of Yarimca station records of 1999 Kocaeli Earthquake (Fig. 3) is utilized as ground motion [28]. This ground motion continued up 35.0 s is applied to

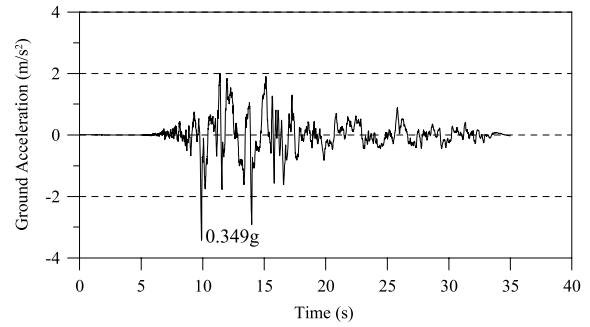


Fig. 3. Acceleration time history of Kocaeli earthquake (YPT330), 1999.

Table 1  
Statistics of the random variables for Jindo Bridge.

Random variable	Substructures	Mean value
Elastic modulus	$E_1$ Cables	$1.5186 \times 10^8$ kN/m <sup>2</sup>
	$E_2$ All elements	$1.9500 \times 10^8$ kN/m <sup>2</sup>
	$E_3$ Girders and towers	$2.0500 \times 10^8$ kN/m <sup>2</sup>
Mass density	$\gamma_1$ Cables	8330 kg/m <sup>3</sup>
	$\gamma_2$ All elements	12 600 kg/m <sup>3</sup>
	$\gamma_3$ Girders and towers	15 570 kg/m <sup>3</sup>

the system in a vertical direction. The dynamic responses of the cable-stayed bridge are obtained for a time interval of 0.005 s.

The cable-stayed bridge is modeled as 169 stochastic finite elements of different length (169 random variables,  $\rho, \sigma = 1, 2, \dots, 169$ ;  $x_\rho$  are ordinates of the element midpoints). MCS method is simulated for 10 000 simulations.

Stochastic analysis of a cable-stayed bridge is performed for earthquake ground motion by taking into account uncertainties of material properties. For this purpose, two different uncertainties of material characteristics are considered. These are elastic modulus and mass density.

*Case I: Random material property is elastic modulus (E)*

The elastic modulus ( $E_3$ ) of 130 elements constituting Jindo Bridge's towers and decks are  $2.05 \times 10^8$  kN/m<sup>2</sup> (Table 1), however, five different elastic modulus belonging to 30 cable elements are changing between  $1.424 \times 10^8$  kN/m<sup>2</sup> and  $1.561 \times 10^8$  kN/m<sup>2</sup>. The perturbation method applied uses only one variable for covariance matrix. On the other hand, MCS method considers each elastic modulus separately. For this reason, when applying perturbation method, firstly it should be determined which variable (elastic modulus) is used to calculate covariance matrix? In this example, the elastic modulus giving the nearest displacement value to the one obtained from MCS method was decided by trying three different elastic modulus. After this process, other steps are continued with the elastic modulus selected. Table 1 presents elastic modulus' statistics used during perturbation method. Here,  $E_1$  express the mean values of cables' elastic modulus. On the other hand,  $E_2$  gives the mean values of all elements (cables, towers and deck).

Coefficient of variation (COV) was selected as  $\alpha = 0.1$  for these random variables [1]. The perturbation based SFEM is very efficient for low material variability. Higher than 0.1–0.15 coefficients of variation (COV) of input random variables demand higher-order Taylor expansion in equilibrium equations and higher-order expansion of the solution [1,3]. The respective expectation and correlation function for the elastic modulus  $E_\rho$  are assumed as follows:

$$\begin{aligned} E[E_1] &= 1.5186 \times 10^8 \\ E[E_2] &= 1.95 \times 10^8 \quad \lambda = 10 \\ E[E_3] &= 2.05 \times 10^8 \end{aligned} \tag{24}$$

$$\mu(E_\rho, E_\sigma) = \exp\left(-\frac{|x_\rho - x_\sigma|}{\lambda l}\right) \tag{25}$$

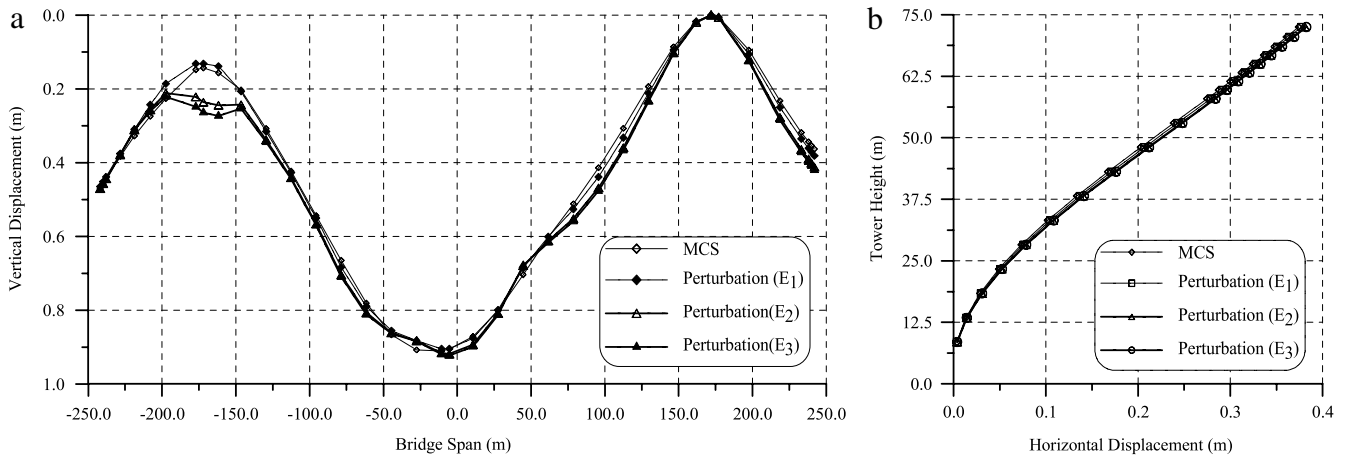


Fig. 4. Maximum vertical displacements at the deck of Jindo Bridge (a) and maximum horizontal displacements along Jindo Island tower (b) for random elastic modulus.

where  $x_\rho$ ,  $l$  and  $\lambda$  are ordinates of the element midpoints ( $n$  random variable,  $\rho, \sigma = 1, 2, \dots, n$ ), structural member length and decay factor.

Case II: Random material property is mass density ( $\gamma$ )

Similar to elastic module's situation, the mass densities are different for cables, decks and towers. The mass density belonging to materials forming the cables is  $8330 \text{ kg/m}^3$  (Table 1). However, the mean value of mass densities of all elements is  $12\,600 \text{ kg/m}^3$ .  $15\,570 \text{ kg/m}^3$  states the mean value of mass densities of towers and decks except for cables as shown in Table 1.

The expectation, correlation function and coefficient of variation of the mass density are given, respectively, as follows:

$$\begin{aligned} E[\gamma_1] &= 8330 \\ E[\gamma_2] &= 12\,600 \quad \lambda = 10 \\ E[\gamma_3] &= 15\,570 \end{aligned} \tag{26}$$

$$\mu(\rho_\rho, \rho_\sigma) = \exp\left(-\frac{|x_\rho - x_\sigma|}{\lambda l}\right) \tag{27}$$

$$\alpha = 0.1.$$

4. Numerical results

4.1. Responses of the Cable-stayed bridge for random elastic modulus

In the first part of this study, cable-stayed bridge responses with respect to random elastic modulus according to perturbation based SFEM and MCS methods are determined compared with each other.

The absolute maximum vertical displacement responses of the bridge deck and horizontal displacements along the Jindo Island tower obtained from perturbation based SFEM and MCS methods for random elastic module are shown in Fig. 4 and Table 2. Two analyses give very close results each other at the middle point of deck and at the top point of tower where maximum displacements occurred. If consider average difference obtained from perturbation method,  $E_1$  gives the best result according to MCS (4.78%) for deck and (1.87%) for tower.

Here, it is seen that the best results are obtained from  $E_1$  value. Therefore, other internal forces (axial forces, shear forces and bending moments) are given for only this elastic module (Figs. 5, 6 and Tables 3, 4).

The maximum axial forces, shear forces and bending moments for deck of the Jindo Bridge are presented in Fig. 5. It is seen from Fig. 5 and Table 3 that values acquired from MCS and perturbation methods are closed to each other. As shown in Table 3, the

minimum differences between the axial forces, shear forces and bending moments of these two methods are 0.12%, 0.07% and 0.18%, respectively. Average differences for these internal forces are about 3.70%, 5.50% and 3.49%, respectively. Also in this table (Table 3), the mean maximum values acquired by the perturbation based SFEM are smaller than those calculated by the MCS method.

Fig. 6 presents axial forces, shear forces and bending moments along tower height for Jindo Island according to MCS method and perturbation based SFEM. The results obtained from the perturbation method are close to the results from MCS method as seen Fig. 6 and Table 4. The minimum absolute differences between these two methods for axial forces, shear forces and bending moments are about 0.57%, 0.13% and 0.12%, respectively. As shown in Table 4, average differences for these internal forces are about 3.52%, 4.60% and 1.32%, respectively. The mean of maximum internal forces calculated by the Perturbation method are compared with those of the maximum values obtained by the MCS dynamic analysis for the Jindo Island tower in Table 4. In addition, here the internal forces obtained by the MCS dynamic analysis are higher than the mean of maximum values by the perturbation method along the tower height.

4.2. Responses of the cable-stayed bridge for random mass density

In the second part of this study, cable-stayed bridge responses for random mass density are calculated and compared with each other according to perturbation based SFEM and MCS methods.

The vertical displacements on the Jindo Bridge deck and the horizontal displacements along the Jindo Island tower obtained from perturbation based SFEM and MCS for random mass density of the cable-stayed bridge system are plotted in Fig. 7. The results obtained from the perturbation method are close to the results from MCS method as seen Fig. 7 and Table 5. Two analyses types gives close results each other at the middle point of deck and at the top point of tower where maximum displacements occurred. If consider average differences obtained from perturbation method,  $\gamma_1$  gives the best result according to MCS for deck (5.66%) and for tower (0.22%).

If the results obtained from these displacements are mentioned; for the SFEM analysis of this bridge system, minimal mass density ( $\gamma_1$ ) gives the nearest results calculated by MCS method. Therefore, other internal forces (axial forces, shear forces and bending moments) are given for this mass density (Figs 8, 9 and Tables 6, 7).

The absolute maximum axial forces, shear forces, bending moments calculated by both perturbation based SFEM, and MCS dynamic analyses for the bridge deck are shown in Fig. 8. It is

**Table 2**  
The results of the vertical displacements at the deck of Jindo Bridge and the horizontal displacements at the Jindo Island tower for different random elastic modulus according to perturbation based SFEM and MCS.

		MCS	Perturbation ( $E_1$ )	Perturbation ( $E_2$ )	Perturbation ( $E_3$ )
Deck	Maximum displacement	0.9103 m	0.9042 m	0.9187 m	0.9234 m
	Average displacement	0.41472 m	0.41535 m	0.43698 m	0.44330 m
	Average difference (According to MCS)		4.78%	12.49%	15.10%
Tower	Maximum displacement	0.3741 m	0.3770 m	0.3813 m	0.3824 m
	Average displacement	0.2068 m	0.2096 m	0.2128 m	0.2137 m
	Average difference (According to MCS)		1.87%	4.04%	4.62%

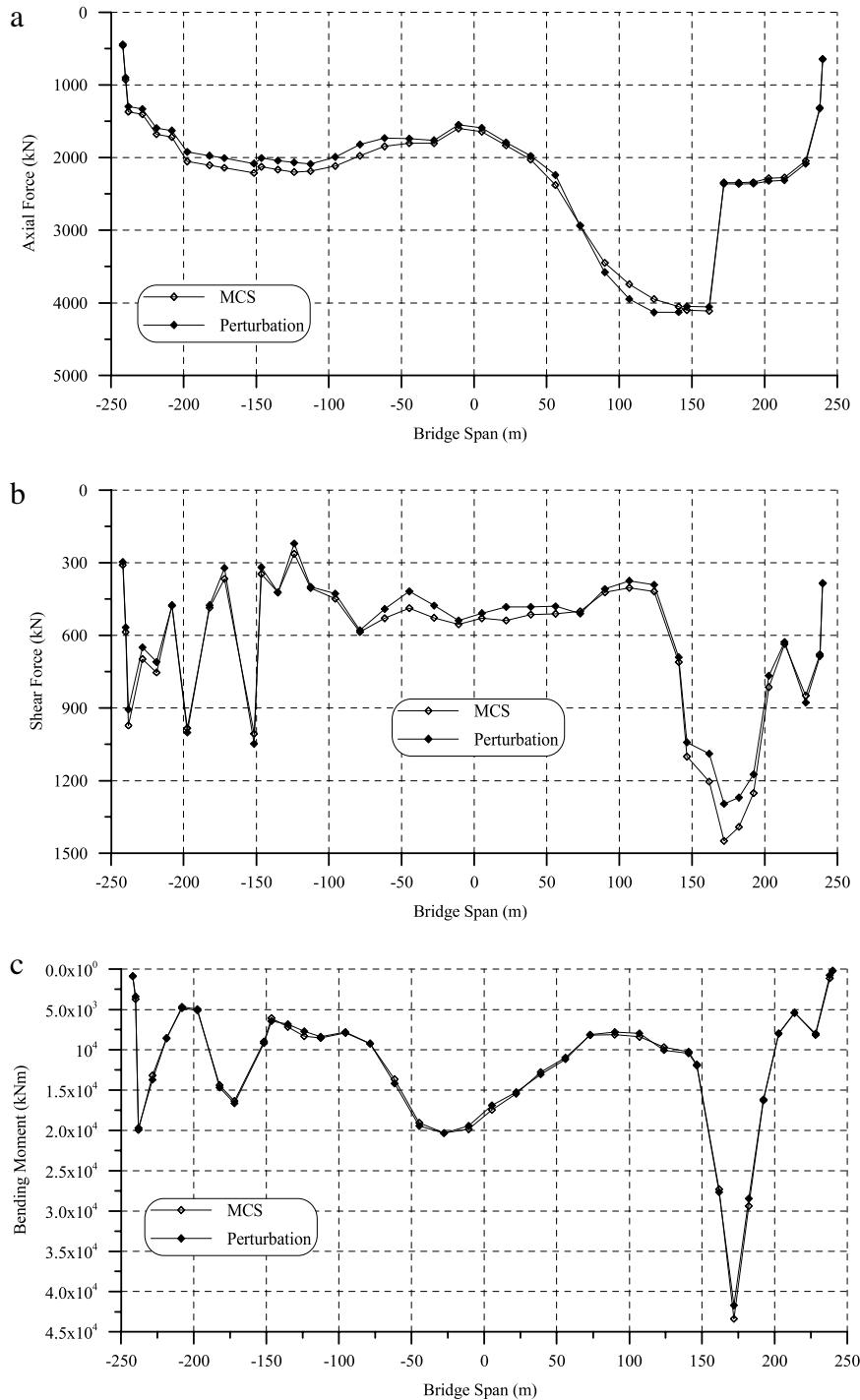


**Fig. 5.** Maximum axial forces (a), shear forces (b) and bending moment (c) for deck of Jindo Bridge for random elastic module ( $E_1$ ).

**Table 3**

The results of axial forces, shear forces and bending moments for deck of Jindo Bridge for random variable  $E_1$ .

		MCS	Perturbation
Axial forces	Maximum axial force	4109.917 kN	4130.062 kN
	Minimum axial force	459.224 kN	442.965 kN
	Average axial force	2197.70 kN	2158.70 kN
	Minimum difference (According to MCS)		0.12%
	Average difference (According to MCS)		3.70%
Shear forces	Maximum shear force	1448.826 kN	1295.944 kN
	Minimum shear force	309.693 kN	296.890 kN
	Average shear force	654.421 kN	622.895 kN
	Minimum difference (According to MCS)		0.07%
	Average difference (According to MCS)		5.50%
Bending moments	Maximum bending moment	43 373.1 kN m	41 705.2 kN m
	Minimum bending moment	188.5 kN m	195.9 kN m
	Average bending moment	12 006.5 kN m	11 927.8 kN m
	Minimum difference (According to MCS)		0.18%
	Average difference (According to MCS)		3.49%

**Table 4**

The results of axial forces, shear forces and bending moments for Jindo Island tower for random variable  $E_1$ .

		MCS	Perturbation
Axial forces	Maximum axial force	4048.311 kN	3891.675 kN
	Minimum axial force	639.235 kN	600.805 kN
	Average axial force	3155.716 kN	3055.149 kN
	Minimum difference (According to MCS)		0.57%
	Average difference (According to MCS)		3.52%
Shear forces	Maximum shear force	988.403 kN	980.378 kN
	Minimum shear force	699.333 kN	675.733 kN
	Average shear force	789.536 kN	755.343 kN
	Minimum difference (According to MCS)		0.13%
	Average difference (According to MCS)		4.60%
Bending moments	Maximum bending moment	34 624.7 kN m	34 346.3 kN m
	Minimum bending moment	482.2 kN m	472.3 kN m
	Average bending moment	12 054.9 kN m	11 985.8 kN m
	Minimum difference (According to MCS)		0.12%
	Average difference (According to MCS)		1.32%

**Table 5**

The results of the vertical displacements at the deck of Jindo Bridge and the horizontal displacements at the Jindo Island tower for different random mass density according to perturbation based SFEM and MCS.

		MCS	Perturbation ( $\gamma_1$ )	Perturbation ( $\gamma_2$ )	Perturbation ( $\gamma_3$ )
Deck	Maximum displacement	0.9124 m	0.9034 m	0.9299 m	0.9361 m
	Average displacement	0.4149 m	0.4116 m	0.4204 m	0.4385 m
	Average difference (According to MCS)		5.66%	7.64%	12.50%
Tower	Maximum displacement	0.3768 m	0.3757 m	0.3810 m	0.3864 m
	Average displacement	0.2081 m	0.2081 m	0.2115 m	0.2251 m
	Average difference (According to MCS)		0.22%	2.06%	4.16%

**Table 6**

The results of axial forces, shear forces and bending moments for deck of Jindo Bridge for random variable  $\gamma_1$ .

		MCS	Perturbation
Axial forces	Maximum axial force	4128.78 kN	4132.06 kN
	Minimum axial force	466.48 kN	443.97 kN
	Average axial force	2177.73 kN	2250.60 kN
	Minimum difference (According to MCS)		0.16%
	Average difference (According to MCS)		4.35%
Shear forces	Maximum shear force	1386.73 kN	1292.61 kN
	Minimum shear force	312.21 kN	298.56 kN
	Average shear force	636.81 kN	625.41 kN
	Minimum difference (According to MCS)		0.06%
	Average difference (According to MCS)		3.88%
Bending moments	Maximum bending moment	43 301.9 kN m	41 100.2 kN m
	Minimum bending moment	180.5 kN m	192.9 kN m
	Average bending moment	12 071.8 kN m	11 644.1 kN m
	Minimum difference (According to MCS)		0.30%
	Average difference (According to MCS)		3.89%



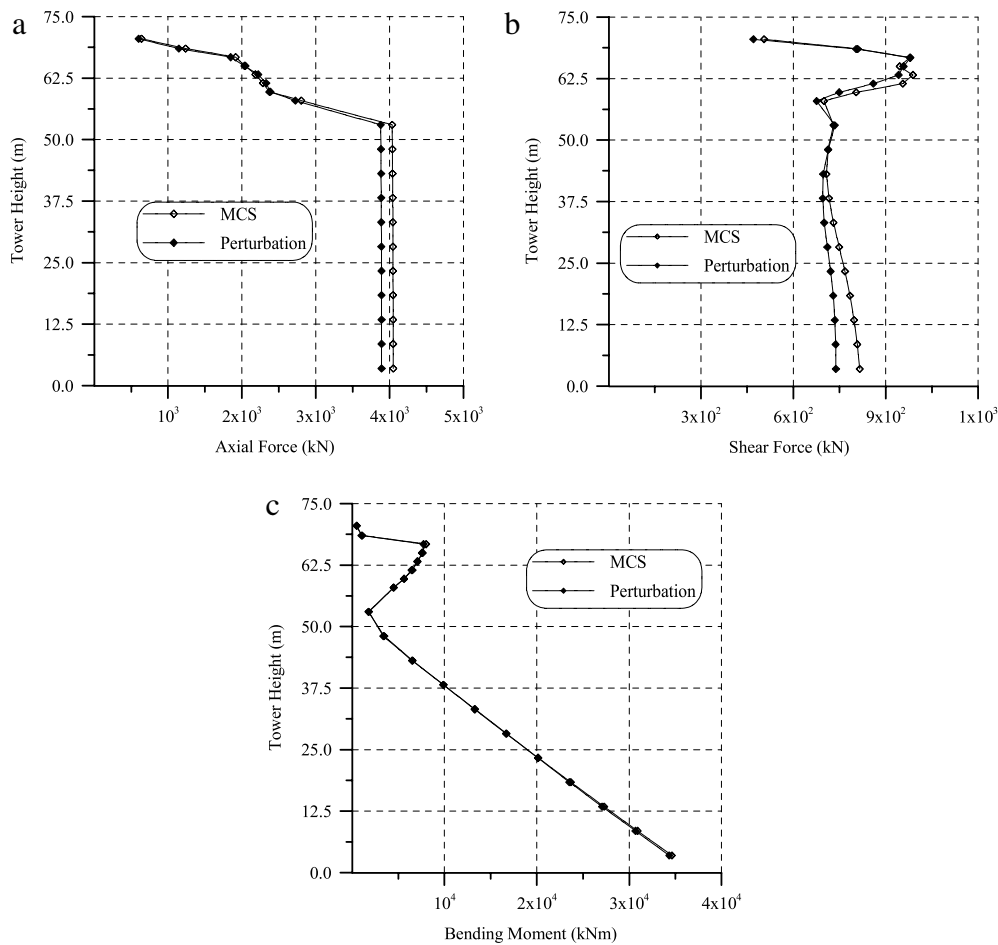


Fig. 6. Maximum axial forces (a), shear forces (b) and bending moment (c) for Jindo Island tower for random elastic module ( $E_1$ ).

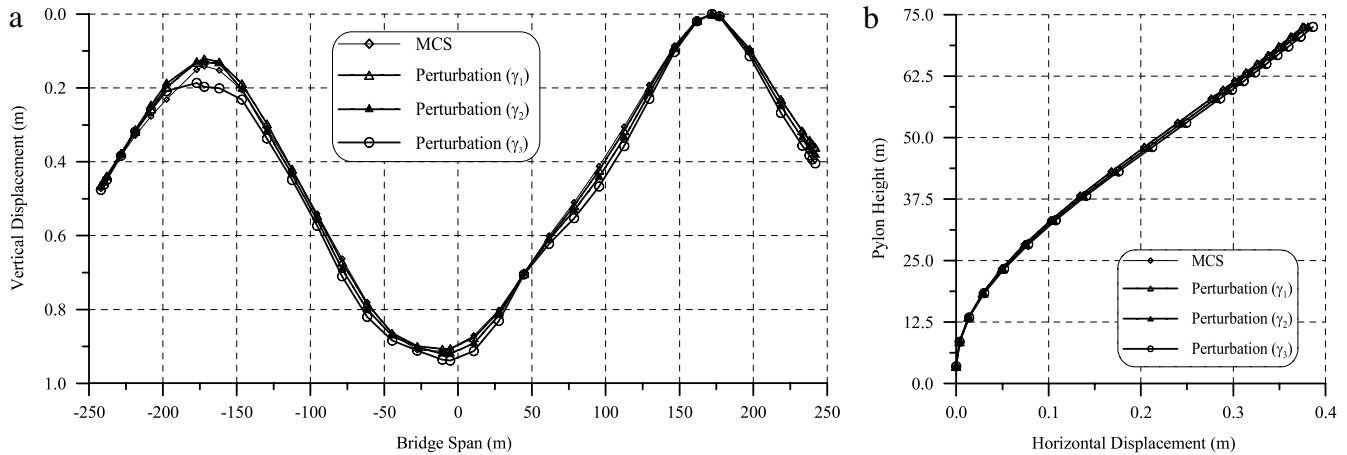


Fig. 7. Maximum vertical displacements at the deck of Jindo Bridge (a) and maximum horizontal displacements along Jindo Island tower (b) for random mass densities.

seen from Fig. 8 and Table 6 that values acquired from MCS are closed to the ones from perturbation method. As shown in Table 6, while minimum differences between the axial forces, shear forces and bending moments of these two methods are 0.16%, 0.06% and 0.30%, respectively, average differences for these internal forces are about 4.35%, 3.88% and 3.89%, respectively. The mean of maximum internal forces obtained from the MCS dynamic analysis are generally higher than the maximum values obtained using perturbation method (Table 6).

The last comparison for random mass density is about the axial forces, shear forces and bending moments for Jindo Island tower as shown in Fig. 9 and Table 7. As shown in Table 7, while minimum

differences between the axial forces of these two methods are 0.12%, average differences are about 3.91%. Also in this table, the minimum absolute differences between these two methods for shear forces and bending moments are about 0.01% and 0.34%, respectively. Average differences for these internal forces are about 3.90%, 2.47% and 1.75%, respectively. The mean maximum values that are obtained from the perturbation based SFEM are smaller than those calculated by the MCS method (Table 7).

If it is mentioned the other results obtained from this example; for the analysis of this bridge system whose numerical properties are presented (Fig. 2), it needs about 5 min for perturbation based stochastic analysis, however, it needs about 8 h for MCS analysis

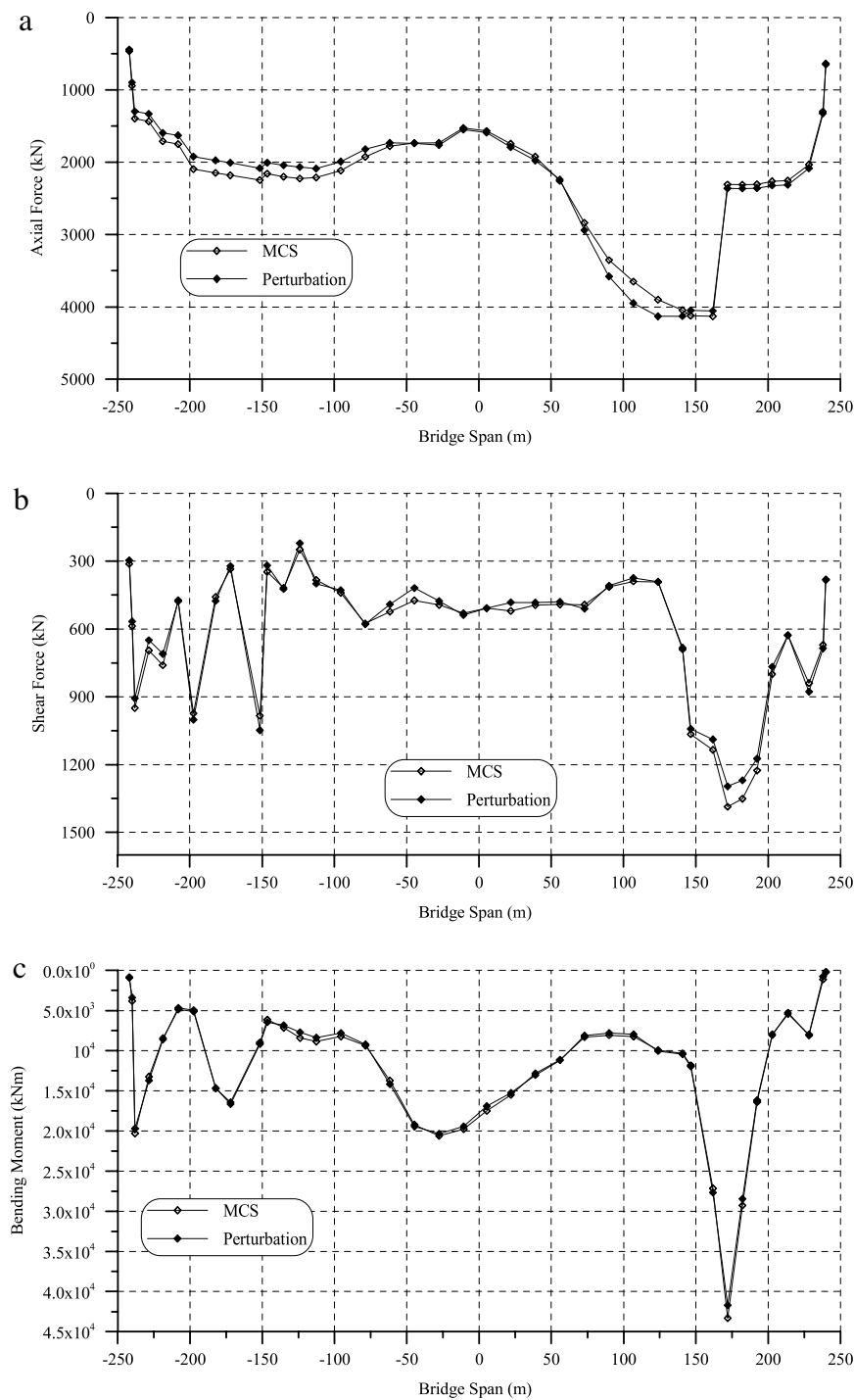


Fig. 8. Maximum axial forces (a), shear forces (b) and bending moment (c) for deck of Jindo Bridge for random mass density ( $\gamma_1$ ).

with the PC which have Intel Pentium (R) 2.40 GHz CPU and 768 MB RAM.

The responses obtained show that selected correlation function suitable for this example for chosen coefficient of variation (COV) value ( $\alpha = 0.10$ ). In addition, the response values obtained from random elastic modulus are generally higher than those from random mass density.

### 5. Conclusions

In this paper, the comparison of the perturbation based SFEM and MCS methods is performed for dynamic responses of a cable-stayed bridge subjected to ground motion. The basic material

properties, such as mass density and modulus of elasticity are supposed to be random variable in the analyses.

The MCS method is a well-known and general methodology that can deal with all classes of engineering problems. It presents, however, high computational cost that has motivated many developments to attempt the reduction of the number of simulations. In practice, all the formulations employ this method as a reference. The SFEM, based on the perturbation technique, offers a very efficient alternative to the MCS method. The numerical application in this study is shown that the perturbation method is able to provide, at an attractive computational cost, a good estimation of the response variability.

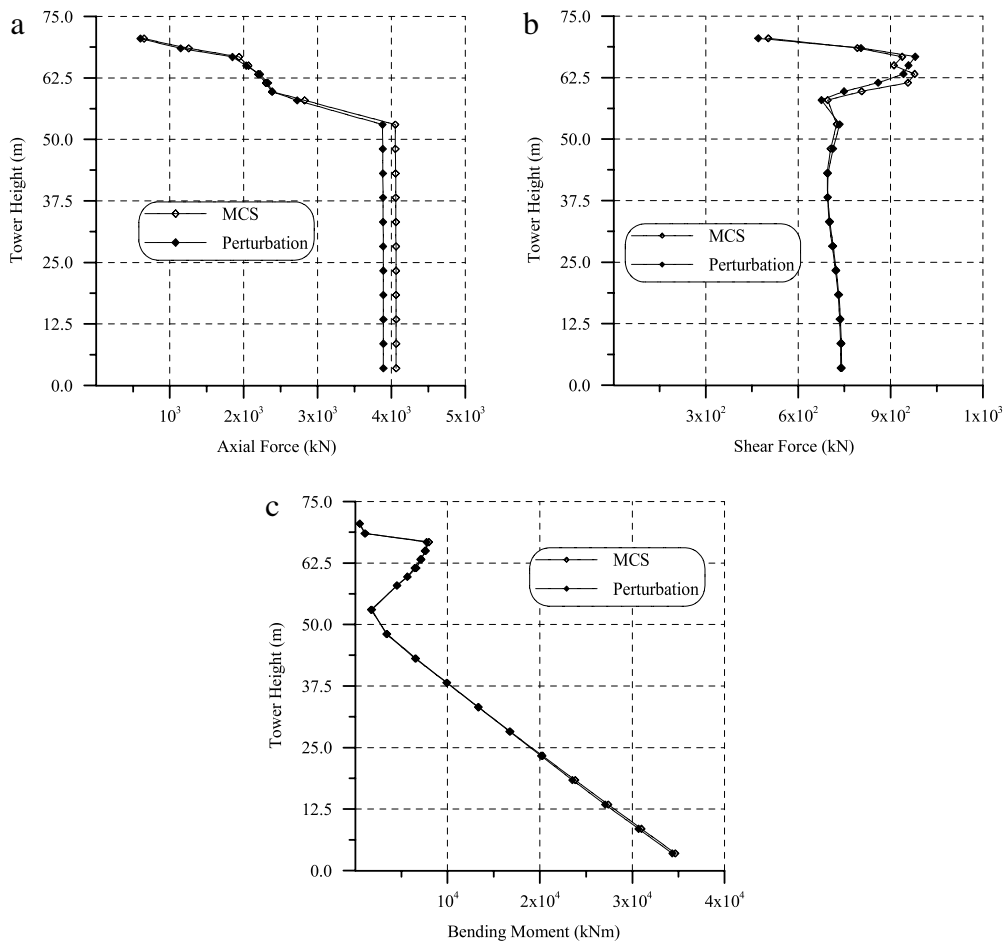


Fig. 9. Maximum axial forces (a), shear forces (b) and bending moment (c) for Jindo Island tower for random mass density ( $\gamma_1$ ).

Table 7

The results of axial forces, shear forces and bending moments for Jindo Island tower for random variable  $\gamma_1$ .

		MCS	Perturbation
Axial forces	Maximum axial force	4065.48 kN	3895.56 kN
	Minimum axial force	648.70 kN	610.81 kN
	Average axial force	3172.49 kN	3076.15 kN
	Minimum difference (According to MCS)		0.12%
	Average difference (According to MCS)		3.90%
Shear forces	Maximum shear force	978.14 kN	967.12 kN
	Minimum shear force	503.08 kN	477.05 kN
	Average shear force	762.73 kN	752.12 kN
	Minimum difference (According to MCS)		0.01%
	Average difference (According to MCS)		2.47%
Bending moments	Maximum bending moment	34664.3 kN m	34202.2 kN m
	Minimum bending moment	476.9 kN m	467.8 kN m
	Average bending moment	12107.2 kN m	11880.5 kN m
	Minimum difference (According to MCS)		0.34%
	Average difference (According to MCS)		1.75%

The presented numerical technique is well suited for computer-aided analysis for structural systems. It was seen that this technique is very suitable for chosen coefficient of variation (COV) value ( $\alpha = 0.10$ ). The perturbation based SFEM should be restricted to applications involving a low variability level of the parameters.

Jindo Bridge modeled in this study, perturbation based SFEM gives close results to MCS method for displacements, axial forces, shear forces and bending moments. Therefore, it can be said that perturbation method could be used instead of MCS method.

Finally, it is observed that the displacement and internal force results in the deck and towers obtained from the perturbation

based SFEM are generally smaller than the mean of maximum values obtained from the MCS method for chosen cable-stayed bridge.

References

- [1] Kleiber M, Hien T. The stochastic finite element method. New York (USA): John Wiley and Sons; 1992.
- [2] Çavdar Ö, Bayraktar A, Çavdar A, Kartal ME. Stochastic finite element analysis of structural systems with partially restrained connections subjected to seismic loads. Steel and Composite Structures 2009;9(6):499–518.
- [3] Melchers RE. Structural reliability analysis and prediction. England: John Wiley & Sons; 1999.

- [4] Yamazaki F, Shinozuka M, Dasgupta G. Neumann expansion for stochastic finite element analysis. *Journal of Engineering Mechanics* 1988;114:1335–54.
- [5] Kaminski M. On generalized stochastic perturbation-based finite element method. *Communications in Numerical Methods in Engineering* 2006;22:23–31.
- [6] Au FTK, Cheung YS, Zheng DY. On the determination of natural frequencies and model shapes of cable-stayed bridges. *Applied Mathematical Modelling* 2001;25:1099–115.
- [7] Baron F, Lien SH. Analytical studies of a cable-stayed girder bridge. *Computers & Structures* 1973;3:443–65.
- [8] Garevski M, Brownjohn JMW, Blakeborough A, Severn RT. Resonance-search tests on a small-scale model of a cable-stayed bridge. *Engineering Structures* 1991;13:59–66.
- [9] Wang PH, Yang CG. Parametric studies on cable-stayed bridges. *Computers & Structures* 1996;60:243–60.
- [10] Abdel-Ghaffar AM, Khalifa MA. Importance of cable vibration in dynamics of cable-stayed bridges. *Journal of Engineering Mechanics, ASCE* 1991;117:2571–89.
- [11] Brownjohn JMW, Lee J, Cheong B. Dynamic performance of a curved cable-stayed bridge. *Engineering Structures* 1999;21:1015–27.
- [12] Fleming JF, Egeseli EA. Dynamic behavior of a cable-stayed bridge. *Earthquake Engineering and Structural Dynamics* 1980;8:1–16.
- [13] Nazmy AS, Abdel-Ghaffar AM. Three-dimensional nonlinear static analysis of cable-stayed bridges. *Computers & Structures* 1990;34:257–71.
- [14] Der Kiureghian A, Ke BJ. The stochastic finite element method in structural reliability. *Probabilistic Engineering Mechanics* 1988;3(2):83–91.
- [15] Dumanoglu AA, Soyluk K. A stochastic analysis of long span structures subjected to spatially varying ground motions including the site-response effect. *Engineering Structures* 2003;25:1301–10.
- [16] Lima BSLP, Ebecken NFF. A comparison of models for uncertainty analysis by the finite element method. *Finite Elements in Analysis and Design* 2000;34:211–32.
- [17] Lei Z, Qiu C. A dynamic stochastic finite element method based on dynamic constraint mode. *Computer Methods in Applied Mechanics and Engineering* 1998;161:245–55.
- [18] Zhu WQ, Wu WQ. A stochastic finite element method for real eigenvalue problem. *Probabilistic Engineering Mechanics* 1992;118:496–511.
- [19] Wang XT, Mei ZX. Random eigenvalue analysis of cooling tower on the spline sub domain random perturbation methods. *Computer Structures Mechanics and Application* 1997;14:174–81.
- [20] Chen JJ, Che JW, Sun HA, Ma HB, Cui MT. Probabilistic dynamic analysis of truss structures. *Structural Engineering and Mechanics* 2002;13:231–9.
- [21] Almansour HH. The performance of hybrid long-span cable stayed bridges using advanced composites. Ph.D. thesis. Department of Civil Engineering, The University of Ottawa; 2006.
- [22] Cheng J, Xiao RC. Probabilistic free vibration and flutter analyses of suspension bridges. *Engineering Structures* 2005;27:1509–18.
- [23] Liu CH, Wang TL, Qin Q. Study on sensitivity of modal parameters for suspension bridges. *Structural Engineering and Mechanics* 1999;8:453–64.
- [24] Shinozuka M. Monte Carlo Simulation of structural dynamics. *Computers & Structures* 1972;2:865–74.
- [25] Zhang J, Ellingwood B. SFEM for reliability of structures with material nonlinearities. *Journal of the Structural Engineering-ASCE* 1996;122:701–4.
- [26] Tappin RGR, Clark PJ. Jindo and Dolsan bridges: Design. *Proceedings of the Institution of Civil Engineers* 1985;78:1281–300.
- [27] Garevski M, Dumanoglu AA, Severn RT. Dynamic characteristics and seismic behavior of Jindo Bridge, South Korea. *Structural Engineering Review* 1988;1:141–9.
- [28] PEER (Pacific Earthquake Engineering Research Centre) 2007. <http://peer.berkeley.edu/smcat/data>.